

Track/Beam	Frame(s)	After image	Before image	B_{\perp}^{**} (m)
288	2453-2471	19 Jul. 1999	22 Oct. 1995	10^1
288	2453-2476	21 Oct. 2002	19 Jul. 1999	200^1
59	2451-2481	17 Jun. 2000	15 Jul. 1992	20
59	2460	26 Aug. 2000	3 Jul. 1999	80
59	2449-2479	13 Apr. 2002	17 Jun. 2000	30^2
6	2453-2541	2 Sep. 2000	4 Jun. 1999	5^3
6	2453-2515	26 Sep. 2000	4 Jun. 1999	40^3
6	2453-2539	18 Aug. 2003	4 Jun. 1999	70^3
6	2453-2515	26 Sep. 2000	2 Sep. 2000	40^3
6	2453-2539	18 Aug. 2003	2 Sep. 2000	60^3
6	2453-2515	18 Aug. 2003	26 Sep. 2000	30^3
7	2470-2484	7 Jun. 2001	12 Jun. 2000	30^3
7	2470-2484	25 Jul. 2001	12 Jun. 2000	60^3
7	2463-2538	15 Jul. 2003	16 Sep. 2000	90^3
7	2463-2538	8 Aug. 2003	16 Sep. 2000	40^3
7	2463-2484	25 Jul. 2001	7 Jun. 2001	30^3
7	2455-2553	8 Aug. 2003	15 Jul. 2003	50^3

Table DR1: Interferograms made in survey of the volcanoes of Kamchatka. Track numbers are from ERS-1/2, but because there are no track numbers for RADARSAT, we list the beam number (all beams are standard). B_{\perp}^{**} is the perpendicular component of the baseline between the satellites. ¹This interferogram is basically unusable, probably because of seasonal decorrelation. ²This interferogram is unusable either because of seasonal decorrelation or because the images are not on the same Doppler ambiguity (although the ERS catalog indicated that they should be). ³The baseline parameters for RADARSAT are known to lower accuracy than for ERS.

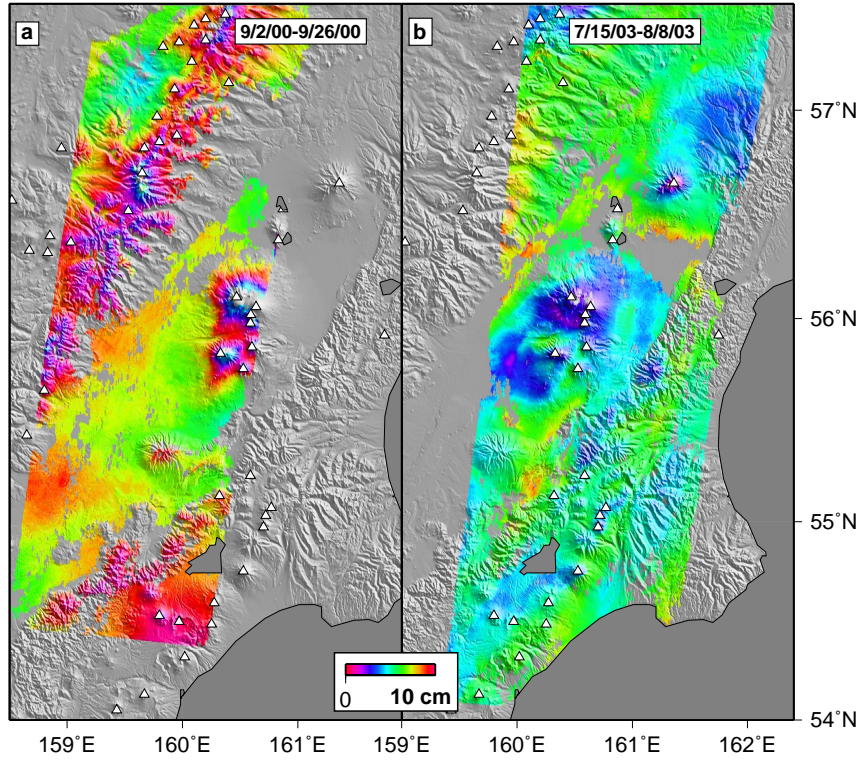


Figure DR1: Interferograms of Kamchatka volcanoes from RADARSAT-1 spanning a single repeat interval (24 days) during the summer showing that most regions remain coherent. There are large phase variations (several cm) related to atmospheric variations. These interferograms have been flattened by assuming no deformation at the 100 km scale, and re-estimating the quadratic baseline parameters to minimize the phase difference between the interferogram and a synthetic interferogram made with a DEM [Rosen *et al.*, 1996]. a. Interferogram spanning 9/26/00-9/2/00 from standard beam 6. b. Interferogram spanning 7/15/03-8/8/03 from standard beam 7.

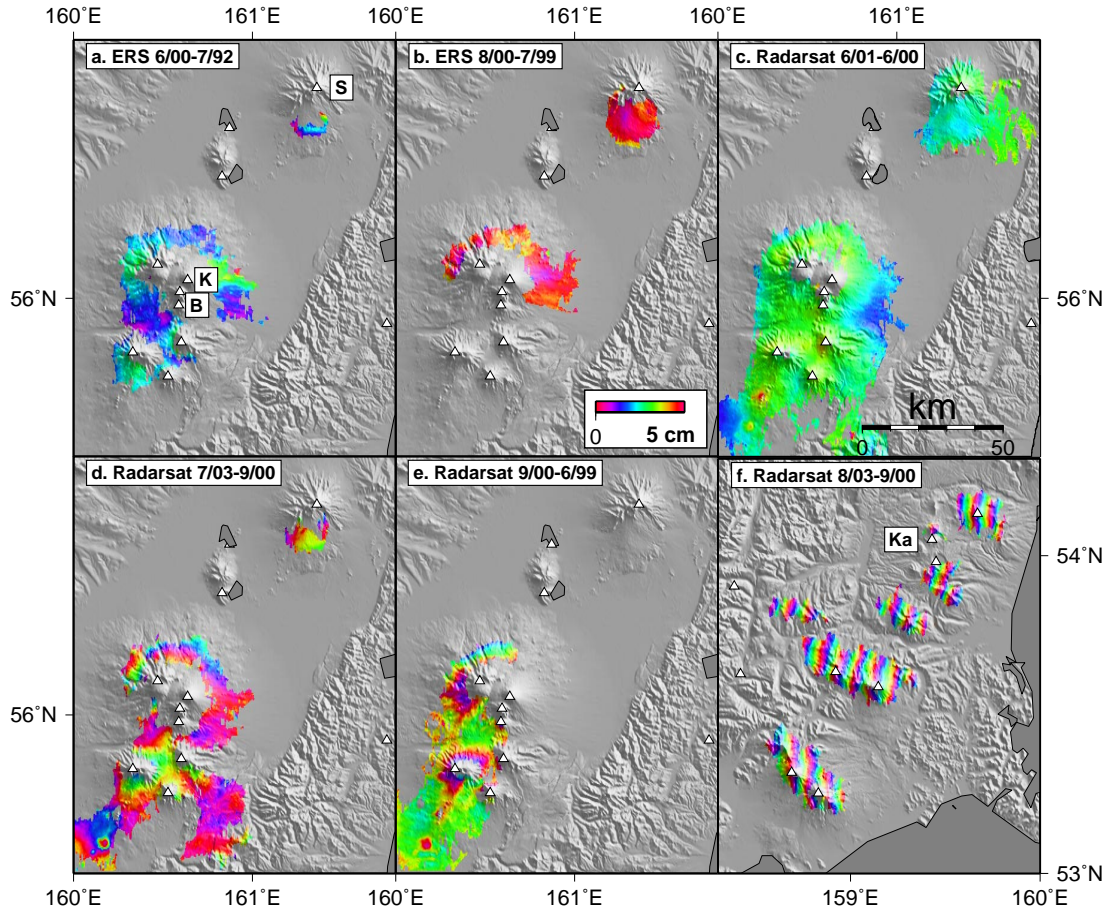


Figure DR2: Co-eruptive interferograms of Kamchatka volcanoes, with Holocene volcanoes. a.-e. Sheveluch and Kliuchevskoi, Bezymianny volcanoes (labeled as S, K and B). All interferograms (except a.) have been empirically flattened with a quadratic ramp to remove orbital errors (see example in f.), allowing for an absolute offset between the Kliuchevskoi group and Sheveluch if necessary. f. The interferogram with the most coherent phase around Karymsky (labeled as Ka), that has not been flattened. Other volcanoes in the area maintain better coherence than Karymsky (other portions of this interferogram are shown in Figure DR2c. and DR2e.). There is no clear deformation in any interferogram related to recent eruptions (see supplemental Table DR2 for more information), although subsidence associated with the 1975-76 New Tolbachik lava flows (see Figure DR2d) is visible in c., d., and e.

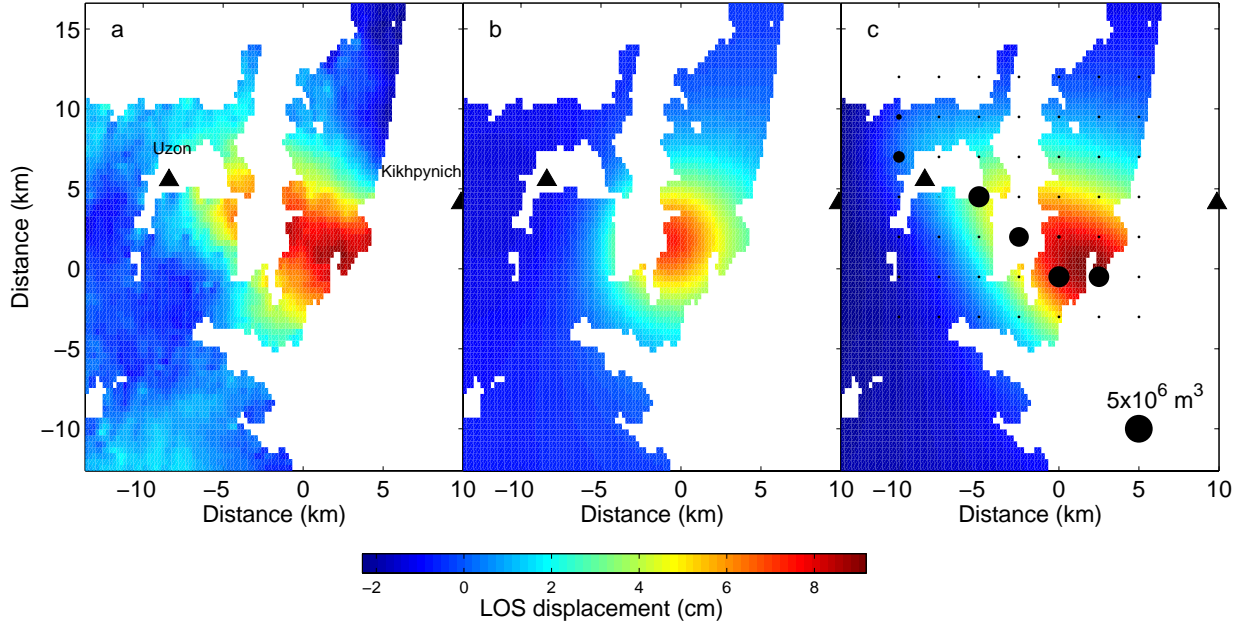


Figure DR3: Here, we show the data for the putative deformation at Uzon caldera, and some preliminary models to illustrate what types of sources would be necessary to explain the deformation. a. Unwrapped interferogram (8/1/8/03-9/2/00, see Figure DR2e). Volcanic edifices are shown as triangles, and the Uzon caldera lies between Uzon and Kikhpynich volcanoes. b. Best fitting spherical point source in a half-space (for technique, see *Pritchard and Simons* [2004]). The volume change is $1 \times 10^7 \text{ m}^3$ and the depth is about 5 km. A spherical source does not well match the observations (the RMS misfit is about 1.2 cm), and so we explore alternative models. c. Model prediction for an array of point sources all fixed at 5 km, but with variable volume change (represented by the size of the circle – volume changes smaller than $1 \times 10^5 \text{ m}^3$ are all the same size). The total volume change is $2 \times 10^7 \text{ m}^3$ and the RMS misfit is 0.95 cm. The volume change was constrained to be positive (using the MATLAB Optimization Toolbox). We explored a variety of point source distributions with variable lateral and depth extent. Better fits to the data can be achieved with arrays of point sources at shallower depths, but in the limit as these sources approach the surface, the result becomes unphysical as each pixel can be explained by a different source. Without other geophysical or geochemical data, it is impossible to determine a robust location for the deforming subsurface reservoirs. A magma chamber was suggested to lie at 5 km depth [Waltham, 2001], but even if true, shallower parts of the geothermal system might also be deforming.

Volcano	Interferograms	Quality	Eruptive episodes**	Figures
Sheveluch	6/17/00-7/15/92	Southermost flank	5	DR2a
	8/26/00-7/3/99	South flank	1	DR2b
	6/7/01-6/12/00	All edifice	1	DR2c
	7/25/01-6/12/00	All edifice	1	N/A
	7/15/03-9/16/00	South flank	1	DR2d
	8/8/03-9/16/00	South flank	1	N/A
Kliuchevskoi	6/17/00-7/15/92	North and east flanks	7	DR2a
	8/26/00-7/3/99	North and east flanks	3	DR2b
	6/7/01-6/12/00	All flanks	1	DR2c
	7/25/01-6/12/00	All flanks	1	N/A
	7/15/03-9/16/00	North and east flanks	3	DR2d
	8/8/03-9/16/00	North and east flanks	3	N/A
Bezymianny	6/17/00-7/15/92	Southwest flank	9	DR2a
	9/26/00-6/4/99	Southwest flank	2	DR2e
	9/2/00-6/4/99	Southwest flank	2	DR2e
	6/7/01-6/12/00	All flanks	2	DR2c
	7/25/01-6/12/00	All flanks	2	N/A
	7/15/03-9/16/00	South flank	4	DR2d
	8/8/03-9/16/00	South flank	5	N/A
Karymsky	8/18/03-9/2/00	North lava flow	1	DR2f
	8/8/03-9/16/00	North lava flow	1	N/A

Table DR2: Compilation of volcanic eruptions that occurred during the timespan of our observations. We did not detect any clear deformation associated with any eruptions, but for most interferograms, only part of the edifice is covered (See Figure DR2), and there is a long timespan allowing any pre-eruptive, co-eruptive and post-eruptive deformation to trade-off perhaps leading to little net deformation. **Several eruptions may have occurred during each eruptive episode, as defined by [Smithsonian Institution, 2004].

References

- Pritchard, M. E., and M. Simons, An InSAR-based survey of volcanic deformation in the central Andes, *Geochem. Geophys. Geosys.*, 5, 10.1029/2003GC000610, 2004.
- Rosen, P. A., S. Hensley, H. A. Zebker, F. H. Webb, and E. J. Fielding, Surface deformation and coherence measurements of Kilauea Volcano, Hawaii, from SIR-C radar interferometry, *J. Geophys. Res.*, 101, 23,109–23,125, 1996.

Smithsonian Institution, Global volcanism report, <http://www.volcano.si.edu>, 2004.

Waltham, T., A guide to the volcanoes of southern Kamchatka, Russia, *Proc. Geologists' Assoc.*, 112, 67–78, 2001.